arXiv:astro-ph/0008452v2 11 Jan 2001

On the coupling between different species during recombination

Steen Hannestad

NORDITA, Blegdamsvej 17, DK-2100 Copenhagen, Denmark

Abstract

Measurements of fluctuations in the Cosmic Microwave Background Radiation (CMBR) is one of the most promising methods for measuring the fundamental cosmological parameters. However, in order to infer parameters from precision measurements it is necessary to calculate the theoretical fluctuation spectrum to at least the measurement accuracy. Standard treatments assume that electrons, ions and neutral hydrogen are very tightly coupled during the entire recombination history, and that the baryon-photon plasma can be treated as a two-fluid system consisting of baryons and photons interacting via Thomson scattering. We investigate the validity of this approximation by explicitly writing down and solving the full set of Boltzmann equations for electrons, ions, neutral hydrogen and photons. The main correction to the standard treatment is from including Rayleigh scattering between photons and neutral hydrogen, a change of less than 0.1% in the CMBR power spectrum. Our conclusion is thus that the standard treatment of the baryon-photon system is a very good approximation, better than any possible measurement accuracy.

Key words: Cosmology: Cosmic microwave background, early universe
PACS: 98.70.Vc, 95.30.Gv, 98.80.-k

1 introduction

Anisotropies in the Cosmic Microwave Background Radiation (CMBR) were first detected in 1992 by the COBE satellite (Smoot et al. 1992). The amplitude and distribution of these temperature fluctuations are closely related to the underlying cosmological model. Thus, a precision measurement of the CMBR fluctuations can in principle yield very precise information about the values of the fundamental cosmological parameters, $\Omega, \Omega_\Lambda, \Omega_b, H_0$ etc. (see for instance Bond et al. 1994, Jungman et al. 1996a,b, Bond, Efstathiou & Tegmark 1997, Eisenstein, Hu & Tegmark 1999). Normally the fluctuations

are parametrized in terms of spherical harmonics as

$$\frac{\Delta T}{T}(\theta,\phi) = \sum_{lm} a_{lm} Y_{lm}(\theta,\phi), \tag{1}$$

where the a_{lm} coefficients are related to the power spectrum by $C_l = \langle a^*_{lm} a_{lm} \rangle_m$. For purely Gaussian fluctuations the power spectrum contains all statistical information about the fluctuations. The data from COBE are not sufficiently accurate for a useful determination of the cosmological parameters. However, a new generation of high-precision experiments will be able to do this. Two balloon experiments, BOOMERANG (de Bernardis et al. 2000) and MAXIMA (Hanany et al. 2000), have already measured the first and second acoustic peaks in the power spectrum (up to $l \lesssim 800$). In the next few years there will be data of even better quality available from the MAP and PLANCK satellite experiments [1]. However, extracting precise information about the cosmological parameters means that we should be able to reliably calculate the theoretical fluctuation spectrum to at least as high precision as that of the best measurement.

Calculating the CMBR power spectrum is a very complicated issue. It involves solving the coupled Boltzmann equations for all different particle species present. This framework has been described in great detail in many papers (see e.g. Ma & Bertschinger 1995), and Hu, Scott, Sugiyama & White (1995) for instance have discussed the influence of various physical assumptions on the final CMBR spectrum.

Since photons exchange momentum and energy with the baryons, a core issue of any CMBR calculation is the treatment of the photon-baryon system. The photons mainly exchange energy with the baryons via Thomson scattering on free electrons. The number of free electrons can be calculated by solving the recombination equations. These equations were first formulated by Peebles (1968) and independently by Zeldovich, Kurt & Sunyaev (1969). Until recently this treatment was used in all calculations of CMBR anisotropies, but it is only accurate to a few percent. Recently Seager, Sasselov & Scott (1999a,b) have provided a much more accurate method for calculating recombination.

However, one assumption which has been made consistently in all treatments is that electrons, protons and neutral hydrogen atoms are very tightly coupled and can exchange energy and momentum much faster than any other relevant timescale (see e.g. Ma & Bertschinger 1995). This means that the photon-baryon system can be treated in a two-fluid approximation, where photons exchange energy with a baryon-fluid which is assumed to have infinitely strong

[1] For information on these missions see the internet pages for MAP (http://map.gsfc.nasa.gov) and PLANCK (http://astro.estec.esa.nl/Planck/).

self-interaction.

In the present paper we calculate interaction and energy-momentum exchange rates for the entire baryon-photon system, and write down the full set of Boltzmann equations for the system of electron, ions, neutrals and photons. Solving this system of equations we find that the assumption of a tightly coupled baryon fluid interacting with photons only through Thomson scattering is a very good approximation, valid at the 10^{-3} level.

In section 2 we calculate the relevant rates for different processes, in section 3 we derive the Boltzmann equations for a multi-fluid baryon plasma, and in section 4 we describe numerical results of solving this extended set of equations. Finally, section 5 contains a discussion of our results.

2 Reaction rates in the photon-baryon plasma

2.1 Photons

Electrons — The main energy exchange mechanism between photons and electrons is Thomson scattering. The scattering rate per photon is given by

$$\Gamma = n_e \langle \sigma_T v \rangle = 1.7 \times 10^{-8}\ \Omega_b h^2 x_e T_{\rm eV}^3\ {\rm s}^{-1}, \tag{2}$$

where $\sigma_T = 8\pi\alpha^2/3m_e^2$ is the Thomson scattering cross-section. Relativistic corrections to the standard cross section are important at the $O(T/m_e) \simeq 10^{-5}$ level (Hu, Scott, Sugiyama & White 1995).

The other main photon-electron processes are bremsstrahlung and double Compton scattering. The rates for these two processes are given roughly by (Hu & Silk 1993a,b, Lightman 1981)

$$\Gamma_{\rm BS} = 3 \times 10^{-15}\ T_{\rm eV}^{5/2} x_e^2 (\Omega_b h^2)^2\ {\rm s}^{-1}. \tag{3}$$

and

$$\Gamma_{\rm DC} = 2 \times 10^{-22}\ T_{\rm eV}^5 x_e (\Omega_b h^2)\ {\rm s}^{-1}. \tag{4}$$

Ions — Photons scatter on ions in exactly the same way as they do on electrons. However, because of the mass difference the cross section is much smaller

$$\sigma = \sigma_T \left(\frac{m_e}{m_p}\right)^2 \simeq 3 \times 10^{-7}\ \sigma_T. \tag{5}$$

Neutrals — Photon scattering on neutrals (Rayleigh scattering) is characterised by the cross section (Jackson 1962, Lightman 1979, Peebles & Yu 1970)

$$\sigma_R = \sigma_T(\omega_\gamma/\omega_0)^4, \;\; \omega_0 = 13.6 \;\; \mathrm{eV}, \tag{6}$$

if $\omega \ll \omega_0$. This cross-section is energy dependent, but the thermal average of the cross section leads to a scattering rate of

$$\Gamma_R = 2 \times 10^{-10} \; \Omega_b h^2 (1 - x_e) T_{\mathrm{eV}}^7 \; \mathrm{s}^{-1}, \tag{7}$$

for $T_{\mathrm{eV}} \lesssim 1$ eV. However, close to the epoch of recombination, the photons are not in scattering equilibrium (Hu & Silk 1993a,b) and the different photon modes do not exchange energy. Therefore the energy dependence of Rayleigh scattering can have different effects in different wavelength bands. We will return to this question in section 5.

2.2 Electrons

Photons — Thomson scattering gives a rate per electron of

$$\Gamma = n_\gamma \langle \sigma_T v \rangle \simeq 1.70 \; T_{\mathrm{eV}}^3 \; \mathrm{s}^{-1}. \tag{8}$$

Ions — Coulomb scattering on ions is characterized by the cross section

$$\sigma_C = \frac{3}{2v^4} \sigma_T \ln \Lambda, \tag{9}$$

where Λ is the Coulomb logarithm

$$\Lambda = \frac{3}{2} \left(\frac{T^3}{\pi \alpha^3 n_e (1 + x_e)} \right)^{1/2}. \tag{10}$$

The scattering rate is then given by

$$\Gamma = n_e \langle \sigma_C v \rangle \simeq \frac{3}{2} \sigma_T \ln \Lambda \left(\frac{m_e}{3T} \right)^{3/2}, \tag{11}$$

and inserting numbers gives a rate of

$$\Gamma = 1.8 \; \log \Lambda \, \Omega_b h^2 x_e T_{\mathrm{eV}}^{3/2} \; \mathrm{s}^{-1}. \tag{12}$$

In addition to Coulomb scattering electrons and ions can recombine to neutral hydrogen. The rate for this process is given roughly by (Lightman 1979, Ma & Bertschinger 1995)

$$\Gamma = 1.7 \times 10^{-7}\ \Omega_b h^2 x_e T_{\rm eV}^{5/2}\ {\rm s}^{-1}, \tag{13}$$

which is entirely negligible as a means of momentum transfer.

Neutrals — Electron scattering on hydrogen atoms at low energy is primarily s-wave, so the cross-section is given by (Mott & Massey 1965)

$$\sigma_N = \frac{4\pi}{k^2}\sum_{l=0}^{\infty}(2l+1)\sin^2\delta_l \simeq \frac{4\pi}{k^2}\sin^2\delta_{l=0} \tag{14}$$

The s-wave phase shift has been calculated for instance by Schwartz (1961). To a reasonable approximation we may put $\delta \simeq \pi$ for $E \ll \omega_0$. In that case the rate is

$$\Gamma = n_n\langle\sigma_N v\rangle \simeq n_n\left\langle\frac{4\pi}{2m_eE_e}\left(\frac{2E_e}{m_e}\right)^{1/2}\right\rangle \tag{15}$$

Inserting numbers into the above equation yields the rate

$$\Gamma = 0.16\ \Omega_b h^2(1-x_e)T_{\rm eV}^{5/2}\ {\rm s}^{-1}. \tag{16}$$

2.3 Ions

We have already seen that Thomson scattering is negligible for protons. The Coulomb scattering rate is the same as for electrons. Scattering on neutrals is very inefficient because of the much higher mass of protons compared with electrons. Finally, the recombination rate is the same for protons as it is for electrons.

2.4 Neutral hydrogen

We shall in the present paper assume that all neutral hydrogen is in the ground state, an approximation which is very good for our purposes.

Photons — The Rayleigh scattering rate has been calculated above to be

$$\Gamma_R = n_\gamma\langle\sigma_R v\rangle \simeq 6.4\times 10^{-3}T_{\rm eV}^7\ \ {\rm s}^{-1} \tag{17}$$

Photo-ionization of neutral hydrogen could in principle also be important. The rate for this process is given by (Ma & Bertschinger 1995)

$$\Gamma = \frac{32}{\sqrt{54}\pi} m_e^{-1/2} T^{3/2} e^4 \left(\frac{T}{B}\right) \phi(T), \tag{18}$$

where B is the binding energy of the given level and $\phi(T) = 0.448 \ln(B/T)$. For ionization from the ground state this is approximately

$$\Gamma = 9.1 \times 10^{10}\ T_{\rm eV} e^{-13.6/T_{\rm eV}}\ {\rm s}^{-1}. \tag{19}$$

Finally, neutral hydrogen can also absorb momentum from the photon gas via photo-excitation. During recombination the Ly-α line is densely populated by resonance photons (Peebles 1968). This effective non-thermal distribution function across the line we denote with f_α. In terms of this the photo-excitation rate from the ground state is

$$\Gamma = 2.1 \times 10^5 f_\alpha T_{\rm eV}^{-1/2}\ {\rm s}^{-1}. \tag{20}$$

From the recombination calculation we find f_α and thus Γ. The system of equations we use is that provided by Peebles (Peebles 1968). Although it is not as accurate as that of Seager, Sasselov & Scott (1999a,b), it is adequate for our purpose. Note that photo-excitation does not in itself transfer any momentum between hydrogen and the other species. Almost all photons in the line are resonance photons and not thermal background photons. However, hydrogen in excited states is ionized almost completely and so the above rate can be seen effectively as the rate for converting hydrogen and *ep*.

Electrons — Scattering on electrons is by far the most important means of exchanging momentum with other species. The rate is roughly given by (c.f. Eq. (16))

$$\Gamma = n_e \langle \sigma_N v \rangle \simeq 0.16\ \Omega_b h^2 x_e T_{\rm eV}^{5/2}\ {\rm s}^{-1}. \tag{21}$$

Ions — Scattering on ions is by s-wave scattering exactly as for electrons. However, the cross section is much smaller because of the much higher mass of protons.

2.5 Ion-electron fluid

The Coulomb interaction between electrons and ions is already the dominant reaction rate in the plasma. However, as soon as there is any motion of

electrons relative to ions, an electric field quickly builds up and acts in the direction opposite to the motion (Hogan 2000). Thus, electrons and ions are even more tightly coupled than the Coulomb scattering suggests and effectively this means that electrons and protons can be treated as one tightly coupled species.

2.6 Comparison of rates

From the above equations we can compare the different rates and identify the dominant ones for momentum exchange between the different species. However, the above equations describe the scattering rates, not the rates for momentum transfer between different species. These two quantities are to a good approximation equivalent, except in the case where photons scatter on massive particles. Because photons have very low momenta compared with massive particles, they are inefficient at transferring momentum to these particles. In each scattering, the photon on average loses a large fraction of its momentum, whereas the massive particle only loses a fraction $\sim T/m$ of its momentum. This effect is only important for the processes described in Eqs. (8) and (17). Both these equations should be multiplied by a factor T/m_p to find the rate of momentum transfer. When this is done, all rates are momentum transfer rates and can be directly compared.

Fig. 1 shows the different rates as a function of time. From the figure it is clear which processes we need to include, they are:
1) Thomson scattering which couples photons with the ion-electron plasma
2) Rayleigh scattering which couples photons with neutral hydrogen
3) s-wave scattering which couples the ion-electron fluid with neutral hydrogen (this process is dominant for $z \lesssim 2000$).

3 Boltzmann equations for a multi-fluid baryon-photon plasma

The evolution of different particle species can be described via the Boltzmann equation. In deriving the equations below we shall work in synchronous gauge because the numerical code for calculating CMBR power spectra, CMBFAST (Seljak & Zaldarriaga 1996), is written in this gauge. As the time variable we use conformal time $d\tau \equiv dt/a(t)$, where $a(t)$ is the scale factor. Finally, instead of using physical momentum, p_j, we work with comoving momentum, $q_j = ap_j$, because it is a conserved quantity in the expanding universe. Finally, we parametrize it as $q_j = qn_j$, where q is the magnitude and n_j is a 3-vector describing its direction. Generically, the Boltzmann equation can always be

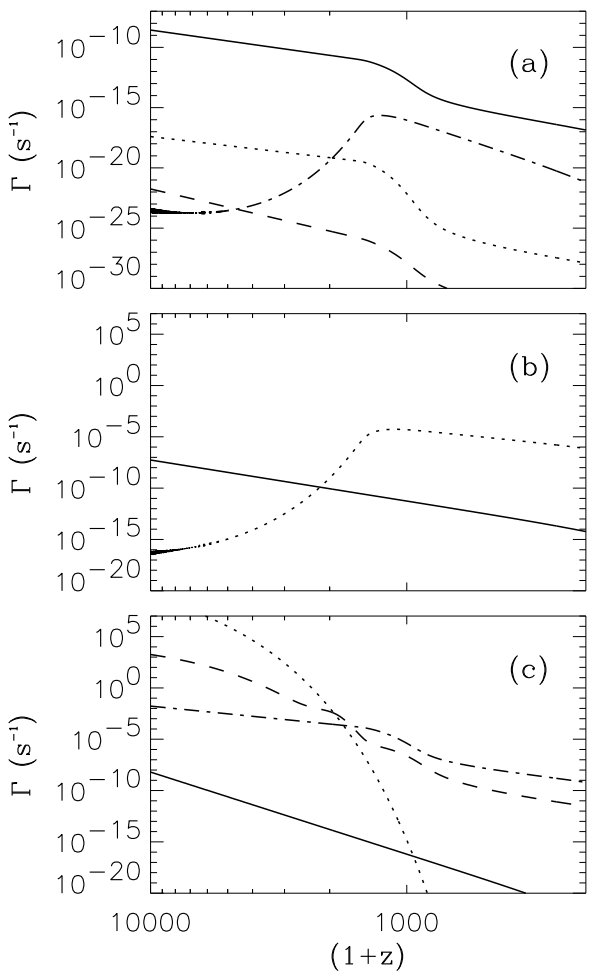

Fig. 1. Momentum transfer rates for the different species present during CMBR formation: (a) photons, (b) ion-electron fluid, (c) neutrals. In each case, the labeling is as follows: (a) Full line is Thomson scattering, dotted is bremsstrahlung, dashed is double Compton scattering and dot-dashed is Rayleigh scattering. (b) Full line is Thomson scattering, dotted is scattering on neutrals. (c) Full line is Rayleigh scattering, dotted is photo-ionization, dashed is photo-excitation and dot-dashed is scattering on electrons. All rates were calculated assuming a standard flat CDM model with $\Omega_m = 1, \Omega_b = 0.05, H_0 = 50\ \mathrm{km\,s^{-1}\,Mpc^{-1}}$.

written as

$$L[f] = \frac{Df}{D\tau} = C[f], \tag{22}$$

where $L[f]$ is the Liouville operator. The collision operator on the right-hand side describes any possible collisional interactions.

We then write the distribution function as

$$f(x^i, q, n_j, \tau) = f_0(q)[1 + \Psi(x^i, q, n_j, \tau)], \tag{23}$$

where $f_0(q)$ is the unperturbed distribution function. f_0 can be found by solving the unperturbed Boltzmann equation (Kaplinghat et al. 1999)

$$\frac{df_0}{d\tau} = C[f_0]. \tag{24}$$

The perturbed part of the Boltzmann equation can be written as an evolution equation for Ψ in k-space (Ma & Bertschinger 1995)

$$\frac{1}{f_0}L[f] = \frac{\partial\Psi}{\partial\tau} + i\frac{q}{\epsilon}\mu\Psi + \frac{d\ln f_0}{d\ln q}\left[\dot{\eta} - \frac{\dot{h}+6\dot{\eta}}{2}\mu^2\right] = \frac{1}{f_0}C[f], \tag{25}$$

where $\mu \equiv n^j\hat{k}_j$. h and η are the metric perturbations, defined from the perturbed space-time metric in synchronous gauge (Ma & Bertschinger 1995)

$$ds^2 = a^2(\tau)[-d\tau^2 + (\delta_{ij} + h_{ij})dx^i dx^j], \tag{26}$$

$$h_{ij} = \int d^3k e^{i\vec{k}\cdot\vec{x}}\left(\hat{k}_i\hat{k}_j h(\vec{k},\tau) + (\hat{k}_i\hat{k}_j - \frac{1}{3}\delta_{ij})6\eta(\vec{k},\tau)\right). \tag{27}$$

Collisionless Boltzmann equation — At first we assume that $\frac{1}{f_0}C[f] = 0$. We then expand the perturbation as

$$\Psi = \sum_{l=0}^{\infty}(-i)^l(2l+1)\Psi_l P_l(\mu). \tag{28}$$

One can then write the collisionless Boltzmann equation as a moment hierarchy for the Ψ_l by performing the angular integration of $L[f]$

$$\dot{\Psi}_0 = -k\frac{q}{\epsilon}\Psi_1 + \frac{1}{6}\dot{h}\frac{d\ln f_0}{d\ln q} \tag{29}$$

$$\dot{\Psi}_1 = k\frac{q}{3\epsilon}(\Psi_0 - 2\Psi_2) \tag{30}$$

$$\dot{\Psi}_2 = k\frac{q}{5\epsilon}(2\Psi_1 - 3\Psi_3) - \left(\frac{1}{15}\dot{h} + \frac{2}{5}\dot{\eta}\right)\frac{d\ln f_0}{d\ln q} \tag{31}$$

$$\dot{\Psi}_l = k\frac{q}{(2l+1)\epsilon}(l\Psi_{l-1} - (l+1)\Psi_{l+1}) \ , \ \ l \geq 3 \tag{32}$$

It should be noted here that the first two hierarchy equations are directly related to the energy-momentum conservation equation. This can be seen in the following way. Let us define the density and pressure perturbations of the dark matter fluid as (Ma & Bertschinger 1995)

$$\delta \equiv \delta\rho/\rho \tag{33}$$
$$\theta \equiv ik_j \delta T^0_j/(\rho + P) \tag{34}$$
$$\sigma \equiv -(\hat{k}_i\hat{k}_j - \frac{1}{3}\delta_{ij})(T^{ij} - \delta^{ij}T^k_k/3). \tag{35}$$

Then energy and momentum conservation implies that (Ma & Bertschinger 1995)

$$\dot{\delta} = -(1+\omega)\left(\theta + \frac{\dot{h}}{2}\right) - 3\frac{\dot{a}}{a}\left(\frac{\delta P}{\delta\rho} - \omega\right)\delta \tag{36}$$
$$\dot{\theta} = -\frac{\dot{a}}{a}(1-3\omega)\theta - \frac{\dot{\omega}}{1+\omega}\theta + \frac{\delta P/\delta\rho}{1+\omega}k^2\delta - k^2\sigma. \tag{37}$$

By integrating Eq. (29) over $q^2\epsilon dq$, one gets Eq. (36) and by integrating Eq. (30) equation over $q^3 dq$ one retrieves Eq. (37).

Collisional Boltzmann equation — The baryon-photon system is coupled by interactions, so $C[f] \neq 0$. In the standard treatment, where all baryons are assumed to be infinitely tightly coupled to each other, there are only two Boltzmann equations, one for the photons and one for the baryons (Ma & Bertschinger 1995). The baryons are highly non-relativistic and we need only consider the first two terms in the Boltzmann hierarchy, corresponding to energy and momentum. For photons many more terms need to be incorporated. However, in the present treatment we suppress writing out explicitly these higher order terms. The collision term for the system has been calculated many times in the literature and the collisional Boltzmann equations are (Ma & Bertschinger 1995)

Baryons:

$$\dot{\delta} = -\left(\theta + \frac{\dot{h}}{2}\right) \tag{38}$$
$$\dot{\theta} = -\frac{\dot{a}}{a}\theta - \frac{\delta P}{\delta\rho}k^2\delta + \frac{4\rho_\gamma}{3\rho_b}an_e\sigma_T(\theta_\gamma - \theta_b). \tag{39}$$

Photons:

$$\dot{\delta} = -\frac{4}{3}\left(\theta + \frac{\dot{h}}{2}\right) \tag{40}$$
$$\dot{\theta} = k^2(\delta_\gamma/4 - \sigma_\gamma) + an_e\sigma_T(\theta_b - \theta_\gamma) \tag{41}$$
$$+ \text{ higher order terms} \tag{42}$$

The full hierarchy can be found for instance in Ma and Bertschinger (1995).

In our case, instead of an infinitely tightly coupled baryon-electron fluid we have three interacting "species": electrons (e), ions (i) and neutrals (n). This means that 4 different Boltzmann hierarchies have to be solved simultaneously. As discussed in section 3, the electrons and ions can be considered as infinitely tightly coupled because of charge neutrality. This ion-electron fluid we denote by the subscript $i-e$. The Boltzmann hierarchy is now

Ion-electron fluid:

$$\dot{\delta} = -\left(\theta + \frac{\dot{h}}{2}\right) + \frac{\dot{\rho}_{i-e}}{\rho_{i-e}}(\delta_n - \delta_{i-e}) \tag{43}$$

$$\dot{\theta} = -\frac{\dot{a}}{a}\theta - \frac{\delta P}{\delta \rho}k^2\delta + \frac{4\rho_\gamma}{3\rho_{i-e}}an_e\sigma_T(\theta_\gamma - \theta_{i-e}) + an_n\langle\sigma_N v\rangle(\theta_n - \theta_{i-e}). \tag{44}$$

Neutrals:

$$\dot{\delta} = -\left(\theta + \frac{\dot{h}}{2}\right) + \frac{\dot{\rho}_n}{\rho_n}(\delta_{i-e} - \delta_n) \tag{45}$$

$$\dot{\theta} = -\frac{\dot{a}}{a}\theta + \frac{\delta P}{\delta \rho}k^2\delta + \frac{4\rho_\gamma}{3\rho_n}an_n\langle\sigma_R\rangle(\theta_\gamma - \theta_n) + an_{i-e}\langle\sigma_N v\rangle(\theta_{i-e} - \theta_n). \tag{46}$$

Photons:

$$\dot{\delta} = -\frac{4}{3}\left(\theta + \frac{\dot{h}}{2}\right) \tag{47}$$

$$\dot{\theta} = k^2(\delta_\gamma/4 - \sigma_\gamma) + an_e\sigma_T(\theta_{i-e} - \theta_\gamma) + an_s\langle\sigma_R\rangle(\theta_n - \theta_\gamma) \tag{48}$$

$$+ \text{ higher order terms} \tag{49}$$

Here $\langle\sigma_R\rangle$ denotes the thermally averaged Rayleigh cross section. In the equations for $\dot{\delta}$ for neutrals and ions, there is a new term appearing because ions and neutrals can interconvert. $\dot{\rho}$ can be found from solving the unperturbed Boltzmann equation (Kaplinghat et al. 1999), which in the present case is the recombination equation.

4 Numerical results

Solving the above system of equations is quite complicated, but we can easily estimate the importance of the different terms. The first important term is the interaction between neutrals and electrons/ions. We can estimate the relative velocity difference between these two components as

$$\frac{\theta_n - \theta_{i-e}}{\theta_n} \simeq \frac{\frac{4\rho_\gamma}{3\rho_{i-e}} n_e \sigma_T}{n_e \langle \sigma_N v \rangle} \simeq 1 \times 10^{-7} T_{\rm eV}^{-3/2} \tag{50}$$

Thus, the relative velocity building up between neutrals and electrons/ions is at most of $O(10^{-7})$. This correction is exceedingly small and we can to a very good approximation treat neutrals and electrons-ions as infinitely tightly coupled. In that case the above system of equations almost reduces to that in the standard treatment

Baryons:

$$\dot{\delta} = -\left(\theta + \frac{\dot{h}}{2}\right) \tag{51}$$

$$\dot{\theta} = -\frac{\dot{a}}{a}\theta - \frac{\delta P}{\delta \rho} k^2 \delta + \frac{4\rho_\gamma}{3(\rho_{i-e} + \rho_n)} a (n_e \sigma_T + n_n \langle \sigma_R \rangle)(\theta_\gamma - \theta). \tag{52}$$

Photons

$$\dot{\delta} = -\frac{4}{3}\left(\theta + \frac{\dot{h}}{2}\right) \tag{53}$$

$$\dot{\theta} = k^2(\delta_\gamma/4 - \sigma_\gamma) + a(n_e \sigma_T + n_n \langle \sigma_R \rangle)(\theta_b - \theta_\gamma) \tag{54}$$

$$+ \text{ higher order terms} \tag{55}$$

Except for the fact that Rayleigh scattering is now included this form is identical to the standard treatment. Note that the polarization terms for photons are different for Rayleigh scattering compared with for Thomson scattering because Rayleigh scattering corresponds to scattering in a dipole field (see e.g. Jackson 1962). However, this is a higher order effect which is we shall not discuss further in the present paper.

Thus, the corrections to the standard treatment come almost solely from including Rayleigh scattering in the calculations of the temperature power spectrum. We have modified the CMBFAST code to include the effect of Rayleigh scattering. In Fig. 2 we show how the CMBR temperature power spectrum

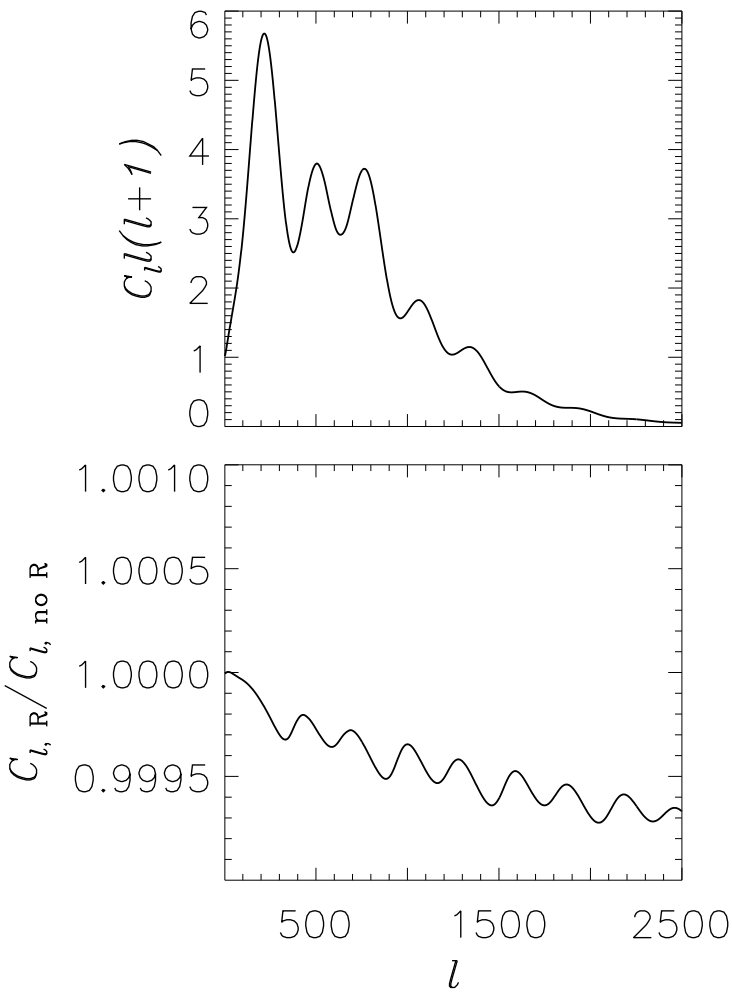

Fig. 2. CMBR power spectra for a standard flat CDM model with $\Omega_m = 1, \Omega_b = 0.05, H_0 = 50\ \mathrm{km\,s^{-1}\,Mpc^{-1}}$, calculated with (full line) and without (dotted line) the inclusion of Rayleigh scattering. The upper panel shows the actual power spectra which are so close that they are indistinguishable on the figure. The lower panel shows the ratio of the two power spectra.

changes due to this inclusion. The difference between the two spectra increases with l, but is always below 10^{-3}. Since the absolute accuracy of CMBFAST is only about 1%, one might worry that the effect is due to numerical noise. However, the effect shown in Fig. 2 is a differential effect, and the accuracy of CMBFAST should therefore be substantially better.

It is in fact possible from analytic arguments, to understand how the inclusion of Rayleigh scattering dampens the fluctuation spectrum. Three effects contribute to change the CMBR power spectrum: 1) Diffusion damping of the perturbations close to recombination is changed by including Rayleigh scattering, 2) The last scattering surface is moved to slightly lower redshift, so that ρ_m/ρ_γ is higher. This means that the early ISW effect is less important, and suppresses power around the horizon size at recombination. 3) Since the

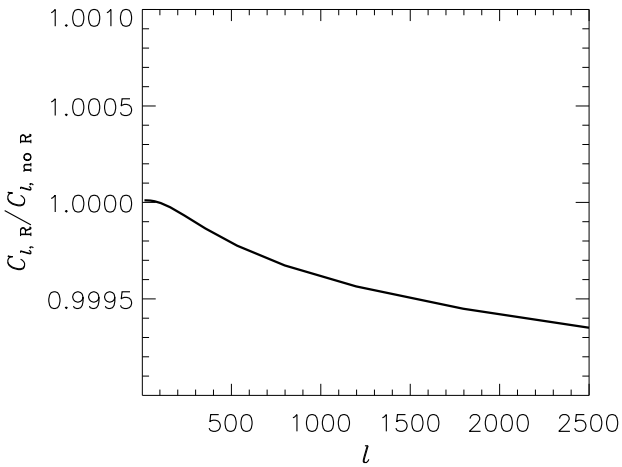

Fig. 3. The damping of the CMBR power spectrum as a function of l, calculated from the analytic estimate of Eq. (58).

last scattering surface is moved to lower redshift, $R \equiv 3\rho_b/4\rho_\gamma$, is also higher. This parameter changes the amplitude of the acoustic oscillations (Hu 1995).

The first effect is the most important and can to a reasonable precision be calculated analytically. The diffusion damping of the k-space fluctuation spectrum can be written roughly as (Hu 1995)

$$P(k)_{\mathrm{damping}} \simeq D^2(k) P(k)_{\mathrm{no\ damping}}, \tag{56}$$

where

$$D(k) = \int_0^{\eta_0} d\eta \dot{\tau} e^{-\tau} e^{-(k/k_D)^2}. \tag{57}$$

Here, $\dot{\tau} = \Gamma$ is the differential optical depth, and $k_D \simeq \int d\eta/\dot{\tau}$ is the diffusion scale for a photon. η is the conformal time coordinate, $d\eta \equiv dt/a$.

We then use the approximate relation that $l \simeq 2k/H_0$ to write that

$$\left(\frac{C_{l,\mathrm{R}}}{C_{l,\mathrm{no\ R}}}\right)_{l \simeq 2k/H_0} \simeq \left(\frac{\int_0^{\eta_0} d\eta \dot{\tau}_R e^{-\tau_R} e^{-(k/k_{D,R})^2}}{\int_0^{\eta_0} d\eta \dot{\tau}_{\mathrm{no\ R}} e^{-\tau_{\mathrm{no\ R}}} e^{-(k/k_{D,\mathrm{no\ R}})^2}}\right)^2 \tag{58}$$

This damping factor is shown as a function of l in Fig. 3. It quite nicely agrees with both the magnitude and shape of the damping seen in the numerically

calculated spectrum (Fig. 2). The oscillatory behaviour of the damping in Fig. 2 comes from the fact that the parameter R is changed (Hu 1995, Landau, Harari and Zaldarriaga 2000), so that the oscillation amplitudes are different when Rayleigh scattering is included.

Thus, the behaviour of the fluctuation damping due to Rayleigh scattering, seen in Fig. 2, is understandable in terms of simple physical arguments.

5 Discussion

We have thoroughly reviewed the interactions between different particle species in the baryon-photon plasma during recombination, as well as written down the complete set of Boltzmann equations for the system of photons, electrons, ions and neutrals. In the standard CMBR calculations, the entire baryon plasma is treated as infinitely tightly coupled to itself. We find that the error introduced by this assumption is only at the 10^{-7} level. The main error in the standard treatment is that Rayleigh scattering between photons and neutral hydrogen is neglected. However, the difference in the power spectrum when this process is included is at most of $O(10^{-3})$, even at high l.

The benchmark for any CMBR calculation is the best possible precision with which any measurement can be made. Because the ensemble average needed in calculating C_l in practise has to be replaced with an average over m there is an uncertainty in C_l of

$$\frac{\sigma(C_l)}{C_l} \geq \sqrt{\frac{2}{2l+1}}, \tag{59}$$

which corresponds to the best precision any CMBR measurement can be made to. Even at $l = 2000$ this "cosmic variance" is $\sigma(C_l)/C_l = 0.022$, which is an order of magnitude higher than the error introduced by neglecting Rayleigh scattering, and several orders of magnitude larger than the error introduced by treating neutrals and ions/electrons as infinitely tightly coupled. Notice, however, that this calculation has been performed using a thermally averaged Rayleigh cross section. Since photons with different energy do not exchange energy at recombination (Hu & Silk 1993a,b), this different Rayleigh interaction rate can lead to different fluctuation spectra in different wavelength bands. A full calculation of this effect requires solving the momentum dependent Boltzmann equation for the photon gas (Ma & Bertschinger 1995), and is beyond the scope of the present work. However, one can get a rough feeling for how the effect of Rayleigh scattering scales with photon energy. In Fig. 4 we show the effect on the power spectrum in the case where the Rayleigh scattering is increased by factors of 2^4 and 3^4 above the value for the average photon

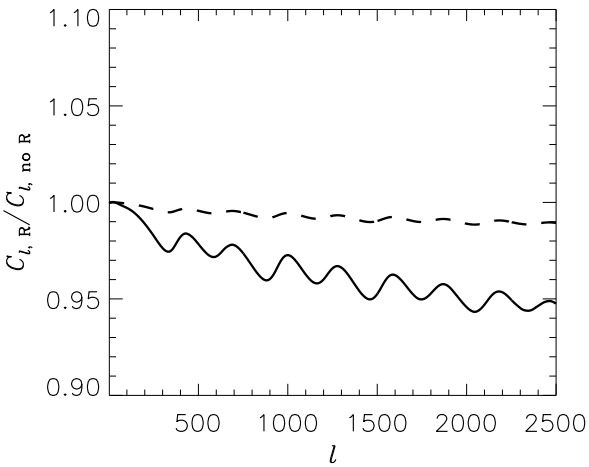

Fig. 4. The damping of the CMBR power spectrum as a function of l, calculated for the cases of $\sigma_R = 2^4\langle\sigma_R\rangle$ (dashed line) and $\sigma_R = 3^4\langle\sigma_R\rangle$ (solid line).

energy. In this case, the effect can be very significant and above the detection threshold. To compare with observations, the highest frequency channel of the Planck surveyor is at 857 GHz (see http://astro.estec.esa.nl/Planck/), which corresponds to $E_\gamma \simeq 15T_0 \simeq 5\langle E_\gamma\rangle$ [2]. So for the Planck surveyor it is not impossible that the effect at high frequencies could be detectable. However, this simplistic analysis clearly overestimates the effect, because increasing the general Rayleigh scattering by a certain amount implicitly assumes that all photons have more energy, which is not really the case. A real calculation using the momentum dependent Boltzmann equation would likely find a somewhat smaller effect, which could nevertheless still be significant at high energy. A second point is that the high frequency bands are subject to heavy foreground contamination (Tegmark et al. 2000), so that a cosmological signal would probably not be visible.

Acknowledgements

Use of the CMBFAST package for calculating CMBR anisotropies (Seljak & Zaldarriaga 1996) is acknowledged.

[2] Note that even though this frequency would from Eq. (6) correspond to $\sigma \simeq 5^4\langle\sigma\rangle$, Eq. (6) does not apply at such high energy during recombination. The upper limit for the cross section would rather be $\sigma \simeq \sigma_T$, which corresponds better to the case of $\sigma = 3^4\langle\sigma\rangle$, shown in Fig. 4.

References

[1] Bernardis P. de, et al., 2000, Nature 404, 955.

[2] Bond, J. R., Efstathiou, G. and Tegmark, M., 1997, Mon. Not. R. Astron. Soc. 291, 33.

[3] Bond, J. R., et al., 1994, Phys. Rev. Lett. 72, 13.

[4] Eisenstein, D. J., Hu, W. and Tegmark, M., 1999, Astrophys. J. 518, 2.

[5] Hanany, S., et al., 2000, astro-ph/0005123.

[6] Hogan, C. J., 2000, astro-ph/0005380.

[7] Hu, W., 1995, PhD Thesis, University of California at Berkeley (astro-ph/9508126).

[8] Hu, W., Scott, D., Sugiyama, N. and White, M., 1995, Phys. Rev. D 52, 5498.

[9] Hu, W. & Silk, J., 1993a, Phys. Rev. Lett. 70, 2661.

[10] Hu, W. & Silk, J., 1993b, Phys. Rev. D 48, 485.

[11] Jackson, J. D., 1962, *Classical Electrodynamics*, John Wiley & Sons.

[12] Jungman, G., et al., 1996a, Phys. Rev. Lett. 76, 1007.

[13] G. Jungman et al., 1996b, Phys. Rev. D 54, 1332.

[14] Kaplinghat, M., et al., 1999, Phys. Rev. D 60, 123508.

[15] Landau, S. J., Harari, D. D. & Zaldarriaga, M., 2000, astro-ph/0010415.

[16] Lightman, A. P., 1981, Astrophys. J. 244, 392.

[17] Lightman, A. P., 1979, *Radiative Processes in Astrophysics*, Wiley Interscience.

[18] Ma, C.-P. & Bertschinger, E., 1995, Astrophys. J. 455, 7.

[19] Mott, N. F. & Massey, H. S. W., 1965, *The Theory of Atomic Collisions*, Oxford Clarendon Press.

[20] Peebles, P. J. E. & Yu, J. T., 1970, Astrophys. J. 162, 815.

[21] Peebles, P. J. E., 1968, Astrophys. J. 153, 1.

[22] Schwartz, C., 1961, Phys. Rev. 124, 1468.

[23] Seager, S., Sasselov, D. D. & Scott, D., 1999a, Astrophys. J. Lett. 523, 1.

[24] Seager, S., Sasselov, D. D. & Scott, D., 1999b, astro-ph/9912182.

[25] Seljak, U. & Zaldarriaga, M., 1996, Astrophys. J. 469, 437.

[26] Smoot, G. F., et al., 1992, Astrophys. J. Lett. 396, L1.

[27] Tegmark, M., Eisenstein, D. J., Hu, W. & Oliveira-Costa, A. de, 2000, Astrophys. J. 530, 133.

[28] Zel'dovich, Ya. B., Kurt, V. G. & Sunyaev, R. A., 1969, Soviet Phys.-JEPT 28, 146.